Scientific Research Publishing

International Journal of Geosciences, 2022, 13, 361-381
https://www.scirp.org/journal/ijg
ISSN Online: 2156-8367
ISSN Print: 2156-8359

Mining Implication in the Geochemical Exploration of Fluvial Sediments of the East Nyambaka Volcanic Zone (Adamawa-Cameroon)

Roland William Edima Yana[1], Augustin Désiré Balla Ondoa[2*], Lise Carole Okomo Atouba[3], Mefire Aminatou Fagny[2], Armel Zacharie Ekoa Bessa[4], Nkouandou Oumarou Faarouk[2]

[1]Centre for Geological and Mining Research, Garoua, Cameroon
[2]Department of Earth Sciences, Faculty of Sciences, University of Ngaoundere, Ngaoundere, Cameroon
[3]Higher Teacher Training College of Bertoua, University of Ngaoundere, Bertoua, Cameroon
[4]Department of Earth Sciences, Faculty of Sciences, University of Yaounde I, Yaounde, Cameroon
Email: *auguste1balla@gmail.com, caroleakam@yahoo.fr, goldrewy@yahoo.com, afagny2002@yahoo.fr, armelekoa@yahoo.fr, ofaarouk@yahoo.fr

How to cite this paper: Edima Yana, R.W., Ondoa, A.D.B., Atouba, L.C.O., Fagny, M.A., Bessa, A.Z.E. and Faarouk, N.O. (2022) Mining Implication in the Geochemical Exploration of Fluvial Sediments of the East Nyambaka Volcanic Zone (Adamawa-Cameroon). *International Journal of Geosciences*, **13**, 361-381.
https://doi.org/10.4236/ijg.2022.135020

Received: January 29, 2022
Accepted: May 28, 2022
Published: May 31, 2022

Abstract

Geochemical characterization in stream sediments from Nyambaka locality was carried out on ten samples collected from the study area watershed. The distribution of trace metals in the sediments showed that some lithophiles (Be, Sc, V, Cr, Sr, Th, U), chalcophiles (Cu, Zn, Ga, As) and siderophiles (Mn, Co, Ni, Mo) have high average contents in the sediments compared to their average concentration in the upper crust. From the factorial analysis of the components, the total variance explained made it possible to represent and capture the main information on the data and to represent them in a graphical frame. Thus, using this graphical frame, the trace elements were divided into four groups opposed to each other. They show an enrichment of stream sediments in group 1 (Cr, Cu, Mn, Be, Ni, Co, Zr, Sr, Ba, Mg) and group 2 (Mo, As, Hg, V, Ag) elements more than group 3 (Ga, Sc, U) and group 4 (Au, Th). Rare earth analysis indicates a high abundance of Lanthanide (28.1 ppm to 42.4 ppm), a high concentration of light rare earth (LREE), and depletion of heavy rare earth (HREE). The variable LREE/HREE ($7.24 < \text{LREE/HREE} < 12.22$) and $(\text{La/Yb})\text{N}$ ($6.70 < (\text{La/Yb})\text{N} < 11.72$) ratios suggest an effect of heterogeneous sorting of heavy minerals with variable enrichment of dense and resistant minerals.

Keywords

Stream Sediments, Geochemistry, Mining Exploration, Volcanic Zone, East

Nyambaka, Cameroon

Highlights

- Lithophiles following, Be, Sc, V, Cr, Sr, Th, U, chalcophiles following Cu, Zn, Ga, As and siderophiles following Mn, Co, Ni, Mo show high average contents in the sediments compared to their average concentration in the upper crust. This seems very interesting for further exploration. Overall, the high trace metal content in stream sediments would be the result of enrichment of the surrounding bedrock and extensive chemical weathering. Thus, the spatial distribution of trace metals is largely controlled by the source geology.
- The component diagram that highlighted the different groups of association between chemical elements in the study area shows that: group 1 elements are opposed to group 3 elements and group 2 elements are opposed to group 4 elements which confirm that the sediments of the creek are much richer in group 1 and 2 elements and less rich in group 3 and 4 elements.

1. Introduction

Stream sediments consist of a mixture of soils and rocks from the watershed upstream of the collection site [1]. They can be inoculated during weathering to the various surface materials. Similarly, the bottoms and geochemical anomalies are associated with different geochemical processes that could be caused by mineralization [2]. Thus, alluvium is generally composed of quartz, feldspars, and mica with minor amounts of heavy minerals such as zircon, rutile, tourmaline, garnet, epidote, and chromium spinel [3]. Their chemical composition depends on the composition of the source rocks and the intensity of chemical alteration, but also mineralogical sorting during transport and deposition [4] [5] [6] [7] [8]. Mobility and redistribution of elements in the secondary environment have been widely used as an exploration tool especially in areas where alteration is intense and/or outcrops are scarce [9]. According to [10], geochemical pattern recognition has been used for many years for geochemical and environmental exploration purposes. For many years, geochemical pattern recognition techniques have been applied to recognize geologic and economic mineral resource information hidden in geochemical data [11]. They have also been used to study the relationships between regional geochemical representations and large ore deposits [12]. In a secondary environment such as stream sediments, local geologic reproductions are related to natural and/or anthropogenic factors [13]. Stream sediments are therefore the primary sample for regional reconnaissance geochemical surveys. It is within this framework that this work is undertaken for the enhancement of the study area, in addition to the results published by [14] in the same area. Stream sediments are widely used to characterize the general geochemistry of watersheds (baseline analysis) to isolate areas with typical geoche-

mistry (anomaly detection). Major, trace, and rare earth elements and their elemental ratios are useful in determining the composition and alteration conditions of the source area [15].

The main objectives of this work are 1) to highlight the average concentration of higher to much higher values of certain elements (Co, Cr, Cu, Ni, Zn, Y, Ga, La, Sn, Sc, Ce) relative to the average concentration of the continental crust; 2) to highlight the mineral occurrence of the study area to consider mineral prospecting in the said locality; 3) to conduct geochemical exploration of REEs and selected metals.

2. Geological and Hydrological Framework

2.1. Geology

The study area is located in the Adamaoua region, between 6˚52' and 6˚60' North latitude and 14˚00' and 14˚8' East longitude. From a structural point of view, the Adamaoua Plateau is part of the great tectonic movements that affected the African continent from the Pan-African orogeny at the end of the Precambrian era, to the opening of the Atlantic Ocean in the Mesozoic. In 1987, Dumont highlighted a WNW-ESE shortening phase (P1) in an unstuck regime that brought into play the dexterous sliding of the N70˚E Pan-African faults, corresponding to the central Cameroonian shears [16]; a NNE-SSW and NW-SE distensive phase (P2) and a NW-SE compressive phase (P3) [17]. The Adamaoua Plateau is a morphostructural unit bounded to the north by the Adamaoua faults and the south by the Djem and Mbere faults (**Figure 1A**).

2.2. Drainage

The study area is covered by two sub-watersheds, namely: the Southern commune watershed (BVSC), which flows to the east of the town of Nyambaka (**Figure 1(B)**), and the Mayo Mambaka watershed (BVMM), which flows to the south towards the large Djérem (Sanaga) collector and corresponds to the low-lying areas. The two watersheds are separated by the National N˚. 1, a natural boundary. The hydrographic network of the study area is dendritic (**Figure 1(B)**), more or less dense, and the rivers belong to two large basins known in Cameroon: the Chad basin and the Atlantic basin.

3. Methodology

A total of 10 stream sediment samples were collected from streams in the Commune's South Watershed (SWW) representing second-order streams. They were collected, at a depth of approximately 0.2 m to 0.4 m on the banks or in the bed of the stream while avoiding disturbed areas. A weight of 3 to 4 kg of raw sample was taken at each location and weighed on an electronic scale (Sartorius and Kitchen scale SF-400), then placed in clean, labeled stainless steel plates and finally air-dried.

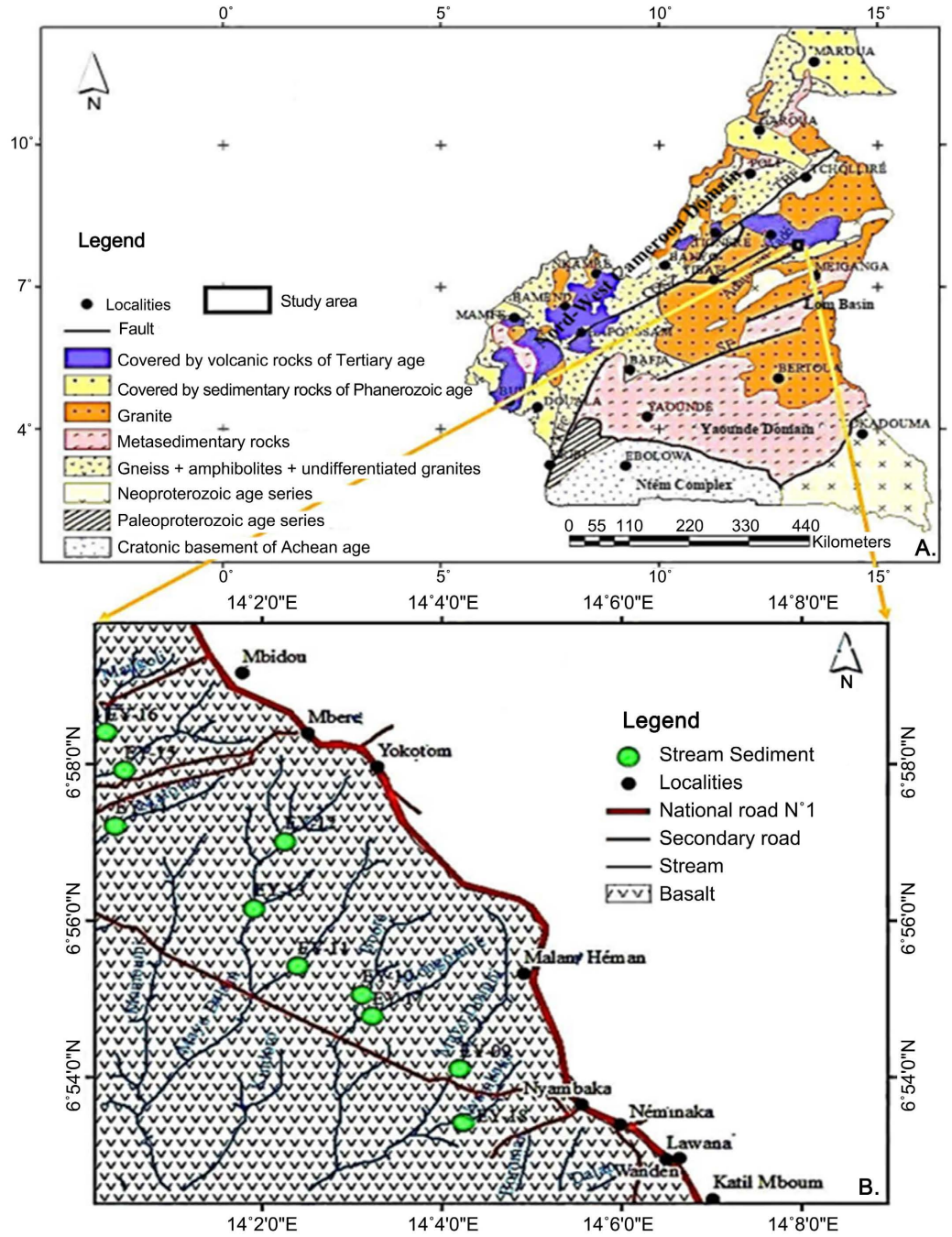

Figure 1. Modified geological map of Cameroon [18]. (a) The major lithological units. AF: Adamaoua Fault; KCF: Kribi-Campo Fault; SF: Sanaga Fault; TBF: Tcholliré-Banyo Fault; (b) Hydrology map of the study area.

In the ore processing laboratory, the samples were ground in a mortar grinder (FRITSCH pulverisette) and 30 g of powder fraction was collected after passing through a 300 μm sieve. This collected pulverized powder fraction was packaged and labeled for analysis. In the laboratory, the samples were dried at a lower temperature 60˚C/140˚F, sieved to −180 micron (80 mesh). The 30 g powder fractions were analyzed by ICP-MS after modified aqua regia digestion, for ul-

tra-low sediment determinations. The twenty (20) chemical elements analyzed, whose detection limit for each is represented in Table 1, will be spatially represented as elements of distribution maps, which plot the occurrence of the geochemistry of the elements superimposed on the drainage, for the geochemical research area.

Data from all river basin samples were combined into a single spreadsheet. The basic descriptive statistic and Pearson's correlation of the content moment were calculated for each river watershed feature. Samples for most locations were at the stream heads and were distributed linearly along the riverbed. The maps were produced using ArcMap.

The standard deviation from the mean of the pooled data was used in assigning color intensities for the maps. This is because it highlights the contrast of high or low values of the population mean. The area is covered by volcanic rocks at the basins. The Pearson correlation coefficient between the average concentration of elements in a particular basin and the area underlain by that rock type in that basin was also calculated. Factor analysis was performed for the same matrix with IBM SPSS Statistics 21 software.

Statistical analyses were performed using Microsoft Excel and SPSS 21.0 for Windows. Statistical parameters such as minimum, median, mean, sum, and maximum were used to measure central tendency; while standard deviation, variance, and coefficient of variance to examine statistical dispersion.

4. Results

4.1. Descriptive Statistics

The results of the descriptive statistics are presented in Table 2. These results were obtained after treatment without logarithmic transformation. The elements Ba, Mo, Cu, Zn, Ni, Co, As, Au, V, and Be show a negative skewness coefficient (<0), hence the negative skewness while the others show a positive skewness.

Table 1. Detection limits of the analyzed chemical elements.

Elements	Units	Detection Limits (L.D)	Elements	Units	Detection Limits (L.D)
Mo	PPM	0.01	**Th**	PPM	0.1
Cu	PPM	0.01	**Sr**	PPM	0.5
Zn	PPM	0.1	**V**	PPM	1
Ag	PPB	2	**Cr**	PPM	0.5
Ni	PPM	0.1	**Mg**	%	0.01
Co	PPM	0.1	**Ba**	PPM	0.5
Mn	PPM	1	**Sc**	PPM	0.1
As	PPM	0.1	**Hg**	PPB	5
U	PPM	0.1	**Ga**	PPM	0.1
Au	PPB	0.2	**Be**	PPM	0.1

Table 2. Descriptive statistics.

	Minimum	Maximum	Average	Standard deviation	median	Skewness	Kurtosis
Cr	302.20	753.60	448.08	128.60	527.90	1.575	3.195
Mg	0.06	0.40	0.21	0.10	0.23	0.608	−0.085
Mn	524.00	1350.00	886.60	300.40	937.00	0.257	−1.339
Ba	84.40	312.80	201.32	79.85	198.60	−0.078	−1.022
Mo	1.36	2.29	1.84	0.29	1.83	−0.142	−0.136
Cu	43.81	54.27	49.69	3.11	49.04	−0.618	0.185
Zn	39.10	98.10	78.21	20.20	68.60	−1.018	−0.047
Ag	15.00	38.00	23.80	6.34	26.50	1.119	2.147
Ni	68.60	273.90	170.92	58.82	171.25	−0.208	0.400
Co	21.70	68.20	45.70	15.47	44.95	−0.304	−0.893
As	1.00	1.70	1.36	0.22	1.35	−0.170	−0.494
U	1.80	3.30	2.47	0.42	2.55	0.317	0.745
Au	0.00	1.50	0.83	0.54	0.75	−0.572	−0.943
Th	11.90	19.10	14.74	2.22	15.50	0.686	0.021
Sr	15.50	113.20	60.38	28.74	64.35	0.410	0.027
V	228.00	295.00	270.00	21.55	261.50	−0.801	−0.066
Sc	26.80	32.10	29.25	1.93	29.45	0.181	−1.233
Hg	16.00	46.00	25.30	9.20	31.00	1.296	1.904
Ga	22.30	34.80	27.03	4.35	28.55	0.535	−0.883
Be	1.40	3.30	2.26	0.58	2.35	−0.064	0.019

Asymmetry: Erreur std = 0.687. Kurtosis: Erreur std = 1.334, N valid (listwise) = 10.

The Kurtosis coefficients of the elements Ba, Mo, Zn, Co, As, Au and V are negative, resulting in a negative skewness or platykurtic distribution. Except for the Kurtosis coefficients of the elements Mg, Mn, Sc, and Ga, which are negative but have a positive skewness (Table 2). For the other elements, they are positive hence the positive skewness or a leptokurtic distribution. In addition, the data set was tested using skewness. Various summary statistics showed that all measured elements were positively skewed. The geochemical data were then log-transformed to obtain a log-normal distribution.

4.2. Geochemistry of Stream Alluvium

Chemical element distribution maps (lithophilic, siderophilic, and chalcophilic) were developed to assess the distribution of chemical elements presented in increasing order of atomic number in stream sediments.

Lithophiles have Be levels recorded in the subwatershed ranging from 1.4 to 3.3 ppm. High Be concentrations (2.3 to 3.3 ppm) are observed in EY-09, EY-10, EY-11, EY-12, and EY-13, medium (1.4 to 2.5 ppm) in EY-16, EY-17, EY-18, and low (1.4 ppm) in EY-14 and EY-15 (Figure 2(A)). The average Be content is

2.26 ppm (Table 2). Recorded Mg contents range from 0.06% to 0.40%. High Mg concentrations (0.25% to 0.40%) are observed in EY-12, medium (0.14% to 0.25%)

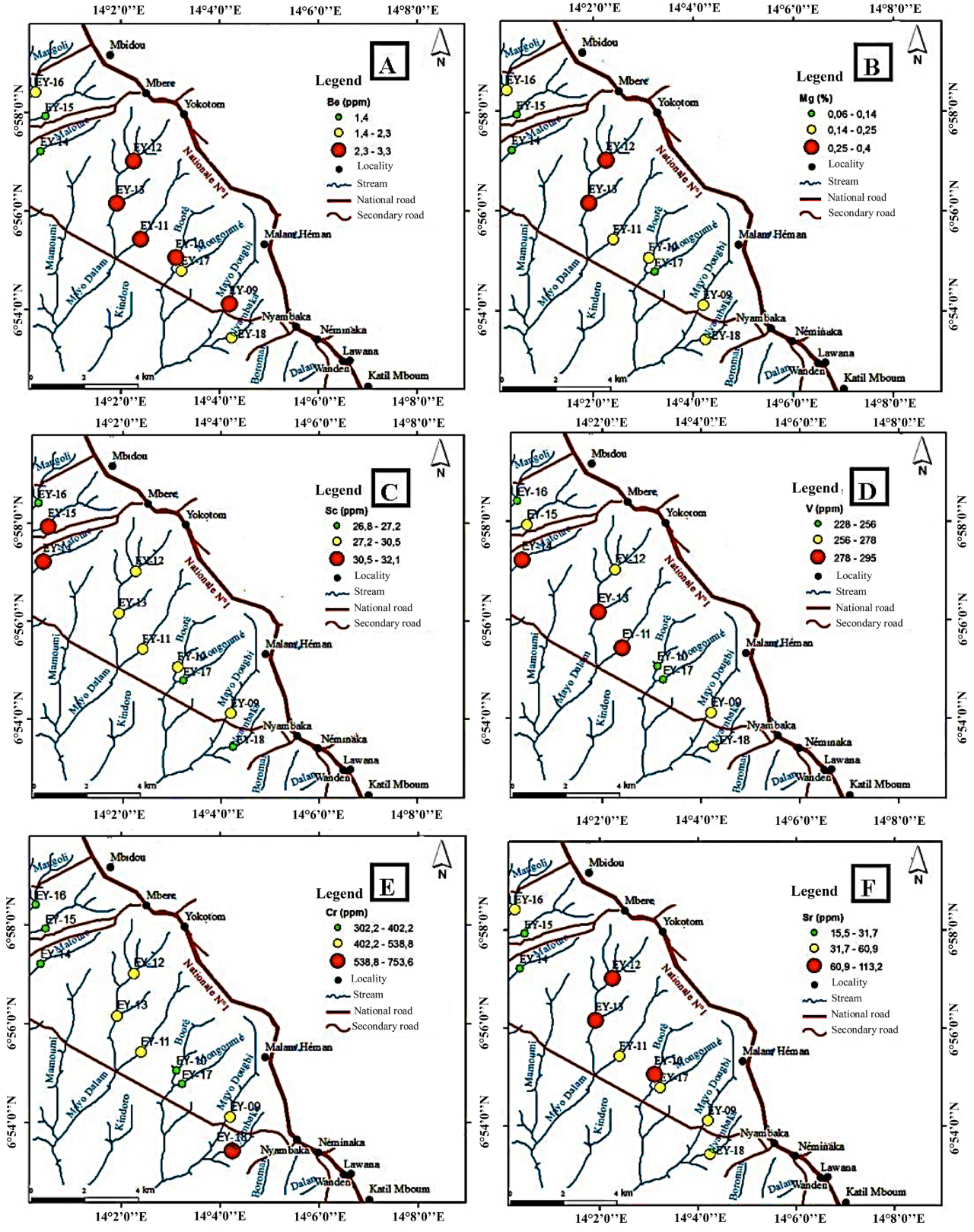

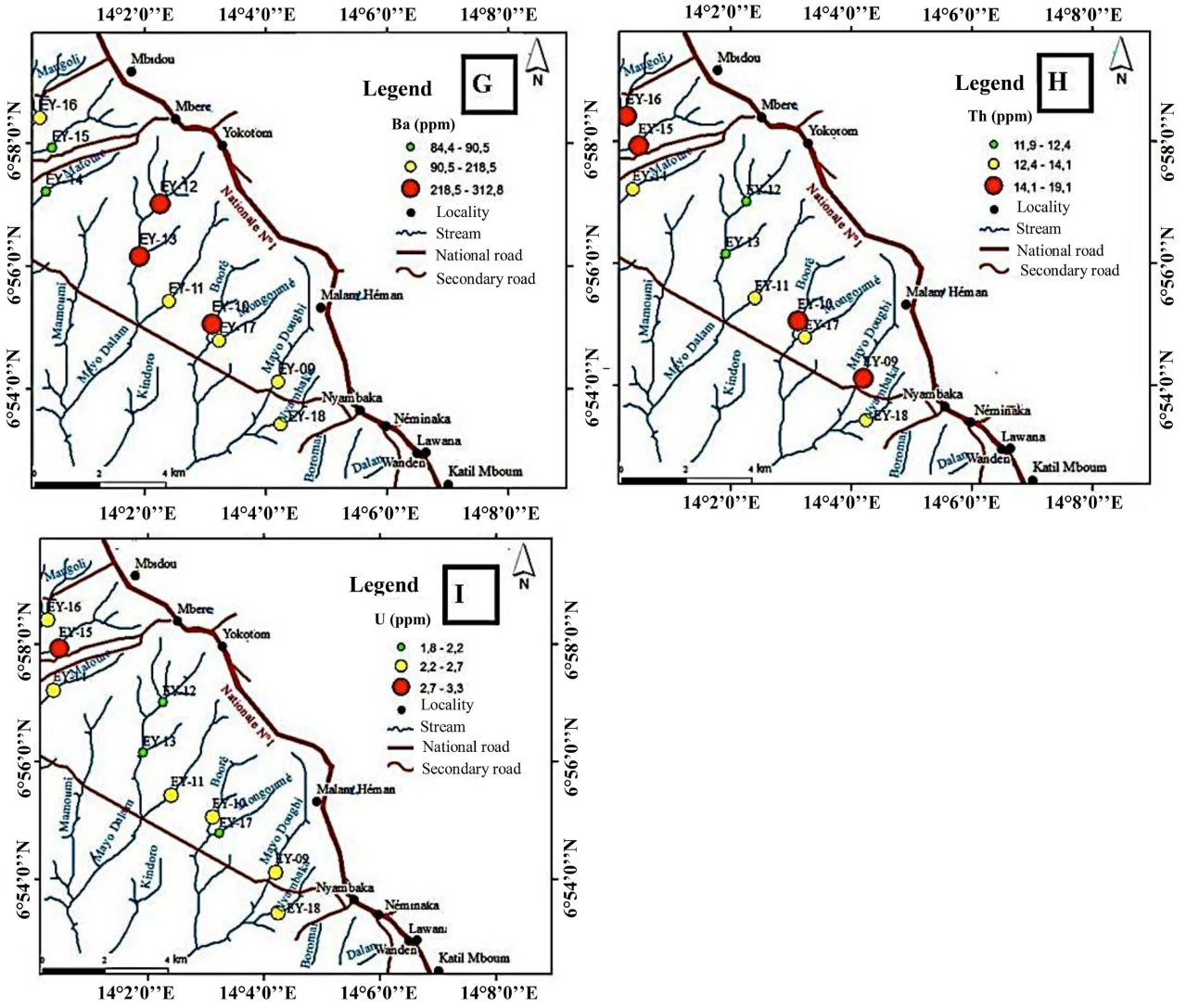

Figure 2. Distribution maps of lithophiles. (A) Be; (B) Mg; (C) Sc; (D) V; (E) Cr; (F) Sr; (G) Ba; (H) Th; (I) U.

in EY-09, EY-10, EY-16, EY-18, and low (0.06% to 0.14%) in EY-14, EY-15 (**Figure 2(B)**). Sc levels recorded range from 26.8 to 32.1 ppm. High Sc concentrations (30.5 to 32.1 ppm) are observed in EY-14, EY-15, medium (27.2 to 30.5 ppm) in EY-09, EY-10, EY-11, EY-12, EY-13, and low (26.8 to 27.2 ppm) in EY-16, EY-17, EY-18 (**Figure 2(C)**). The average Sc content is 29.25 ppm (**Table 2**). V levels recorded in the subwatershed range from 228 to 295 ppm. High V concentrations (278 to 295 ppm) are observed in EY-11, EY-13, EY-14, medium (256 to 278 ppm) in EY-09, EY-12, EY-15, EY-18, and low (228 to 256 ppm) in EY-10, EY-16, EY-17 (**Figure 3(D)**). The average V content is 270 ppm (**Table 2**). The recorded Cr levels range from 302.2 to 753.6 ppm. High Cr concentrations (538.8 to 753.6 ppm) are observed in EY-18, medium (402.2 to 538.8 ppm) in EY-09, EY-11, EY-12, EY-13, and low (302.2 to 402.2 ppm) in EY-10, EY-14, EY-15, EY-16, EY-17 (**Figure 2(E)**). The average Cr content is 448.08 ppm. Sr records from 15.5 to 113.2 ppm. High Sr concentrations (60.9 to 113.2 ppm) are

observed in EY-10, EY-12, EY-13, medium (31.7 to 60.9 ppm) in EY-09, EY-11, EY-16, EY-17, EY-18, and low (15.5 to 60.9 ppm) in EY-14, EY-15 (**Figure 2(F)**). The average Sr content is 60.38 ppm. Ba levels range from 84.4 to 312.8 ppm. High Ba concentrations (218.5 to 312.8 ppm) are observed in EY-10, EY-12, EY-13, medium (90.5 to 218.5 ppm) in EY-09, EY-11, EY-16, EY-17, EY-18, and low (84.4 to 90.5 ppm) in EY-14, EY-15 (**Figure 2(G)**). The average Ba content is 201.32 ppm. Th contents range from 11.9 to 19.1 ppm. High Th concentrations (14.1 to 19.1 ppm) are observed in EY-09, EY-10, EY-15, EY-16; medium (12.4 to 14.1 ppm) in EY-11, EY-14, EY-17, EY-18; and low (11.9 to 12.4 ppm) in EY-12, EY-13 (**Figure 2(H)**). The average Th content is 14.74 ppm. U contents recorded range from 1.8 to 3.3 ppm. The high U concentration (2.7 to 3.3 ppm) is observed in EY-15; the medium ones (2.2 to 2.7 ppm) in EY-09, EY-10, EY-11, EY-14, EY-16, EY-18, and the low ones (1.8 to 2.2 ppm) in EY-12, EY-13, EY-17 (**Figugre 2(I)**). The average U content is 2.47 ppm.

Siderophiles have Mn levels recorded in stream sediments range from 524 to 1350 ppm. High Mn contents (1088 to 1350 ppm) are observed in EY-10, EY-13, medium (641 to 1088 ppm) in EY-11, EY-12, EY-17, EY-18, and low (524 to 641 ppm) in EY-09, EY-14, EY-15, EY-16 (**Figure 3(A)**). The average Mn content is 886.60 ppm (**Table 2**). Co contents recorded ranged from 21.7 to 68, 2 ppm. High Co contents (54.2 to 68.2 ppm) are observed in EY-10, EY-13, medium (39.2 to 54.2 ppm) in EY-11, EY-12, EY-16, EY-18, and low (21.7 to 39.2 ppm) in EY-09, EY-14, EY-15, EY-17 (**Figure 3(B)**). The average Co content is 45.7 ppm. Ni contents recorded here range from 68.6 to 273.9 ppm. High Ni contents (180 to 273.9 ppm) are observed in EY-10, EY-12, EY-13, EY-18, medium (95 to 180 ppm) in EY-09, EY-11, EY-16, EY-17, and low (68.6 to 95 ppm) in EY-14, EY-15 (**Figure 3(C)**). The average Ni content is 170.92 ppm. Recorded Mo ranges from 1.36 to 2.29 ppm. High Mo contents (1.96 to 2.29 ppm) are observed in EY-09, EY-11, medium (1.45 to 11.96 ppm) in EY-10, EY-12, EY-13, EY-14, EY-15, EY-18, and low (1.36 to 1.45 ppm) in EY-16, EY-17 (**Figure 3(D)**). The average Mo content is 1.83 ppm. Recorded Au contents range from 0 to 1.5 ppb. High Au contents (0.8 to 1.5 ppb) are observed in EY-13, EY-14, EY-15, EY-18, medium (0.4 to 0.8 ppb) in EY-09, EY-16, and low (0 to 0.4 ppb) in EY-10, EY-11, EY-12 (**Figure 3(E)**). The average Au content is 0.83 ppb.

Chalcophiles are also variable in content. Recorded Cu ranges from 43.81 to 54.27 ppm. High Cu contents (50.00 to 54.27 ppm) are observed in EY-11, EY-12, EY-13, medium (45.78 to 50.00 ppm) in EY-09, EY-10, EY-14, EY-18, and low (43.81 to 45.78 ppm) in EY-16, EY-17 (**Figure 4(A)**). The average Cu content is 49.69 ppm. Zn levels recorded in stream sediments range from 39.1 to 98.1 ppm. High Zn contents (80.9 to 98.1 ppm) are observed in EY-09, EY-10, EY-12, EY-16, medium (51.1 to 80.9 ppm) in EY-11, EY-17, EY-18, and low (39.1 to 51.1 ppm) in EY-14, EY-15 (**Figure 4(B)**). The average Zn content is 78.21 ppm. Ga contents range from 22.3 to 34.8 ppm. High Ga contents (27.9 to 34.8 ppm) are observed in EY-09, EY-14, EY-15, medium (23.3 to 27.9 ppm) in

EY-10, EY-11, EY-18, and low (23.3 ppm) in EY-12, EY-13, EY-16, EY-17 (Figure 4(C)). The average Ga content is 27.03 ppm. The recorded As contents range

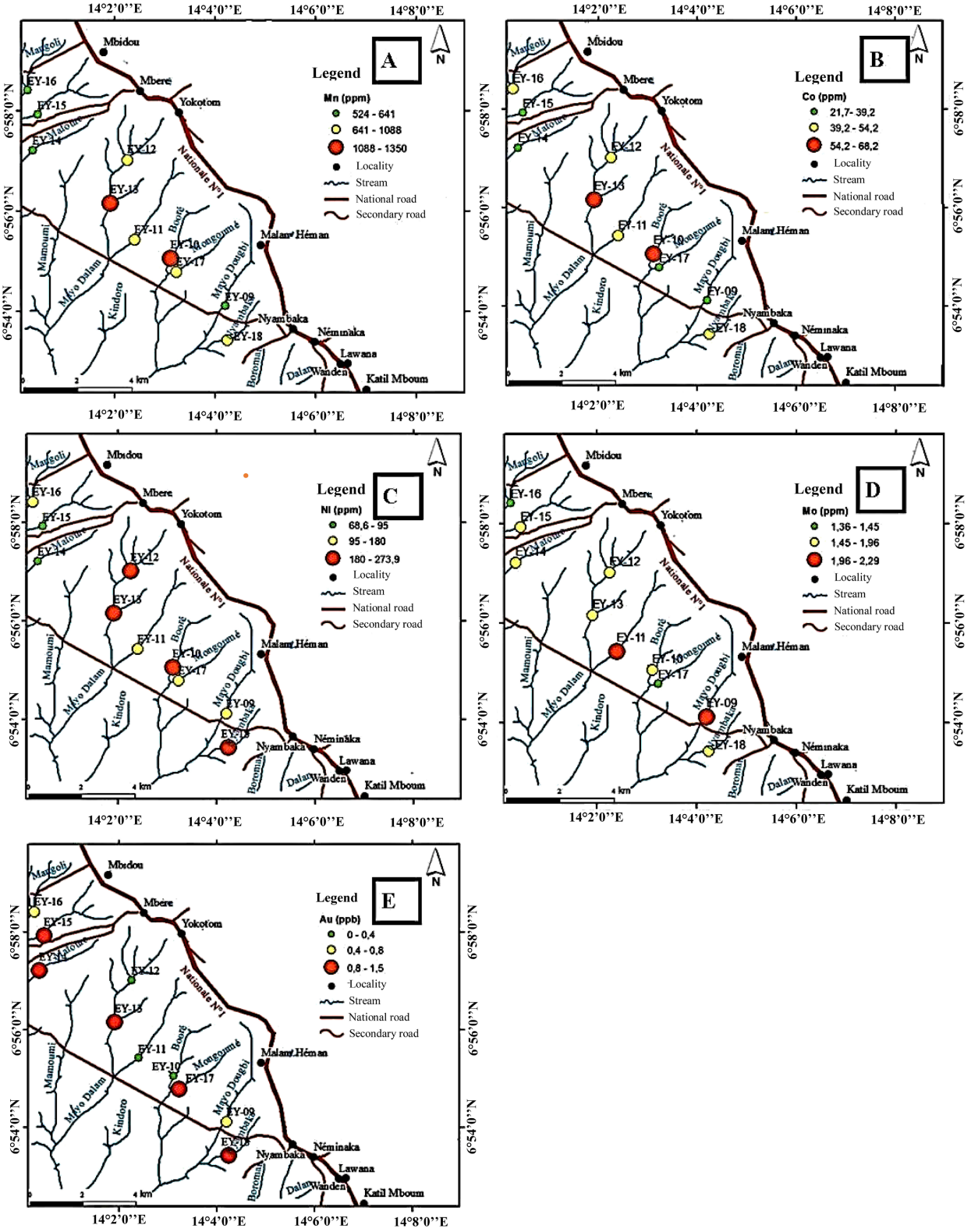

Figure 3. Distribution maps of siderophiles. (A) Mn; (B) Co; (C) Ni; (D) Mo; (E) Au.

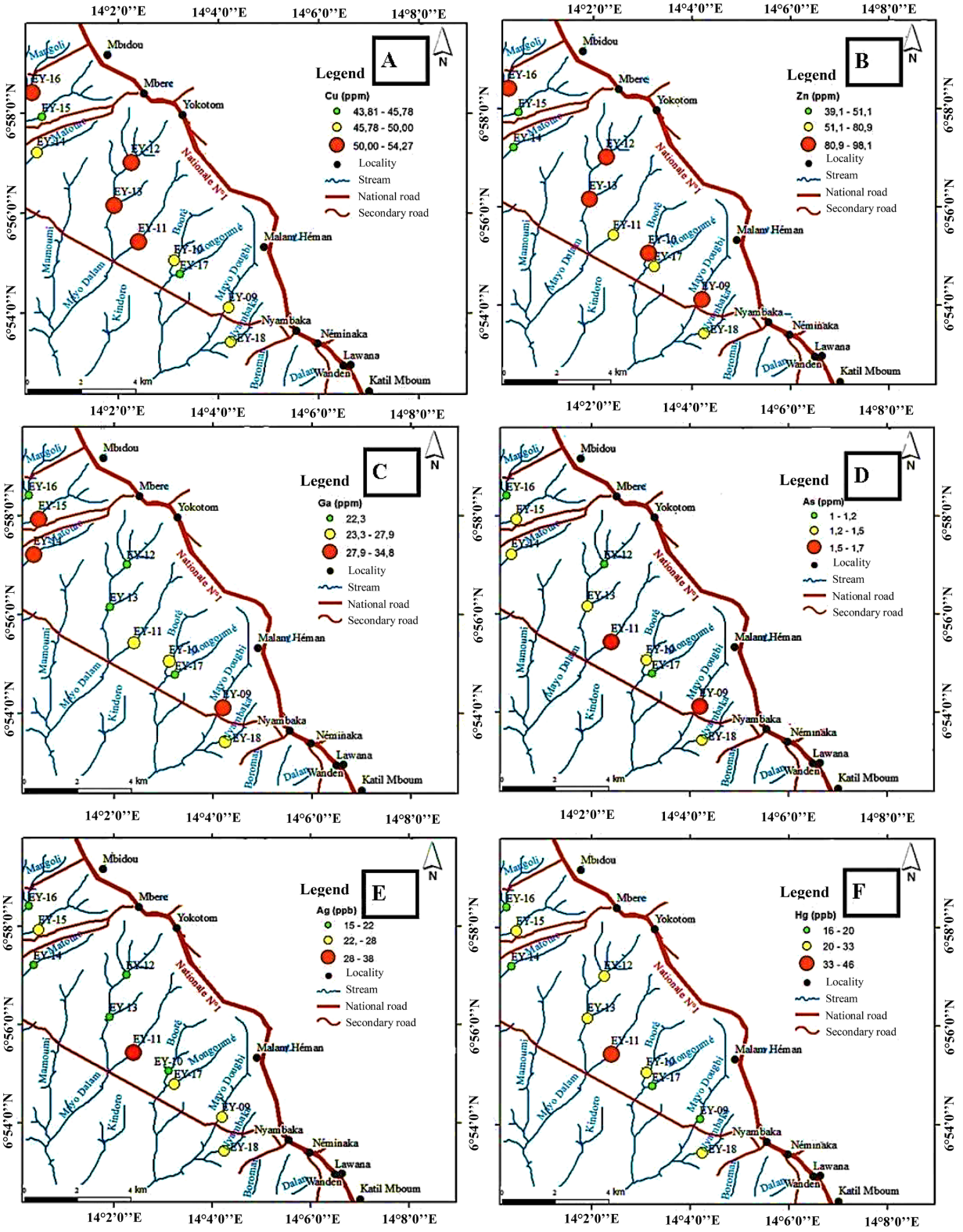

Figure 4. Distribution map of chalcophiles.

from 1 to 1.7 ppm. High As contents (1.5 to 1.7 ppm) are observed in EY-09, EY-11, medium (1.2 to 1.5 ppm) in EY-10, EY-13, EY-14, EY-15, EY-18, and low

(1 to 1.2 ppm) in EY-12, EY-16, EY-17 (Figure 4(D)). The average As content is 1.3 ppm. Ag levels recorded in stream sediments range from 15 to 38 ppb. The high Ag content (28 to 38 ppb) is observed in EY-11; medium (22 to 28 ppb) in EY-09, EY-15, EY-7, EY-18 and low (15 to 22 ppb) in EY-10, EY-13, EY-12, EY-14, EY-16 (Figure 4(E)). The average Ag content is 23.80 ppb. Hg contents recorded range from 16 to 46 ppb. The high Hg content (46 ppb) is observed in EY-11, medium (20 - 33 ppb) in EY-10, EY-12, EY-13, EY-15, EY-18, and low (16 - 20 ppb) in EY-09, EY-14, EY-16, EY-17 (Figure 5(F)). The average Hg content is 25.30 ppb.

4.3. Factor Analysis

Factor analysis was applied on the log-transformed of the geochemical data to deduce the driving factors associated with the multi-elements with the watershed and mineralization. Five factors explaining approximately 91.87% of the variance were generated (Table 3).

Table 3. Component matrix after rotation (Varimax).

Component matrix after rotation (Varimax)					
	Components				
	1	2	3	4	5
Sr	**0.922**	−0.034	−0.125	0.025	0.193
Zn	**0.922**	−0.147	−0.082	−0.116	0.196
Be	**0.921**	0.106	0.079	−0.209	0.034
Ba	**0.909**	−0.211	−0.145	0.126	0.215
Co	**0.888**	−0.195	0.193	0.134	0.179
Mg	**0.860**	−0.229	−0.239	0.279	0.007
Cu	**0.763**	0.111	0.187	0.294	−0.120
Au	**−0.728**	−0.202	−0.418	−0.035	0.274
Ga	**−0.695**	**0.680**	0.076	−0.151	0.024
Mn	**0.685**	−0.067	0.265	0.252	0.400
Ni	**0.657**	−0.293	0.128	0.134	**0.639**
U	**−0.578**	0.368	0.290	**−0.537**	−0.282
Mo	−0.038	**0.944**	0.229	0.126	0.069
As	0.112	**0.840**	0.459	0.055	0.209
Sc	−0.380	**0.794**	−0.078	0.049	−0.434
Ag	−0.064	0.087	**0.956**	−0.015	0.149
Hg	0.081	0.347	**0.887**	0.137	−0.018
Th	−0.129	−0.082	−0.097	**−0.937**	−0.211
V	−0.019	**0.652**	0.113	**0.730**	0.128
Cr	0.100	0.210	0.076	0.284	**0.885**

Rotation method: Varimax with Kaiser normalization. Extraction method: Principal component analysis. a. The rotation converged in 7 iterations.

Factor 1 accounted for 45.145% of the total variability. This factor showed high loadings greater than or equal to the absolute value of 0.5 for Sr, Zn, Be, Ba, Co, Mg, Cu, Au, Ga, Mn, Ni and U. Factor 2 accounted for 22.977% of the total variability. This factor showed positive and high to medium loadings for Ga, Mo, As, Sc, V. Sediments derived from granitic and other felsic rocks [19]. High Factor Scores for these elements report the presence of chalcopyrite (Cu) in the study area. Factor 3 accounts for 10.489% of the total variability. This factor showed positive and high loadings for chalcophiles (Ag, Hg). Factors 4 and 5 account for 8.147% and 5.111% respectively of the total variability.

4.4. Principal Component Analysis (PCA)

Twenty (20) items were subjected to principal component factor analysis in IBM SPSS Statistica 21.0 and all of these items were extracted by this method. The majority of the correlation matrix values are positive and greater than 0.50 except for Cr, Ag, and Th (**Table 4**). The representational qualities of the elements have extraction values that allow representativeness of all extracted values. The total variance explained allowed the majority of the information on the data to be represented and captured and plotted on two axes. In this watershed, 45.146% of the variance of the information is carried by component 1 (X-axis), and 22.977% of the variance is carried by component 2 (Y-axis). Thus, the two axes hold 68.123% of the variance in information for this watershed. The component matrices explain how each element is represented on each axis or component (**Figure 5**).

The component diagram allowed to highlight the different groups of association between chemical elements (**Figure 5**). These are:

- Group 1: Zn-Ni-Cu-Mn-Mg-Co-Be-Ba-Cr-Sr;
- Group 2: Mo-V-As-Hg-Ag;
- Group 3: Ga-Sc-U;
- Group 4: Au-Th.

Table 4. Elements extracted in representation quality.

	Quality of representation				
	Initial	Extraction		Initial	Extraction
Cr	1	**0.274**	As	1	0.900
Mg	1	0.823	U	1	0.651
Mn	1	0.719	Au	1	0.501
Ba	1	0.930	**Th**	1	**0.299**
Mo	1	0.835	Sr	1	0.819
Cu	1	0.604	V	1	0.626
Zn	1	0.830	Sc	1	0.640
Ag	1	**0.368**	Hg	1	0.642
Ni	1	0.739	Ga	1	0.888
Co	1	0.889	Be	1	0.648

Extraction method: Principal component analysis.

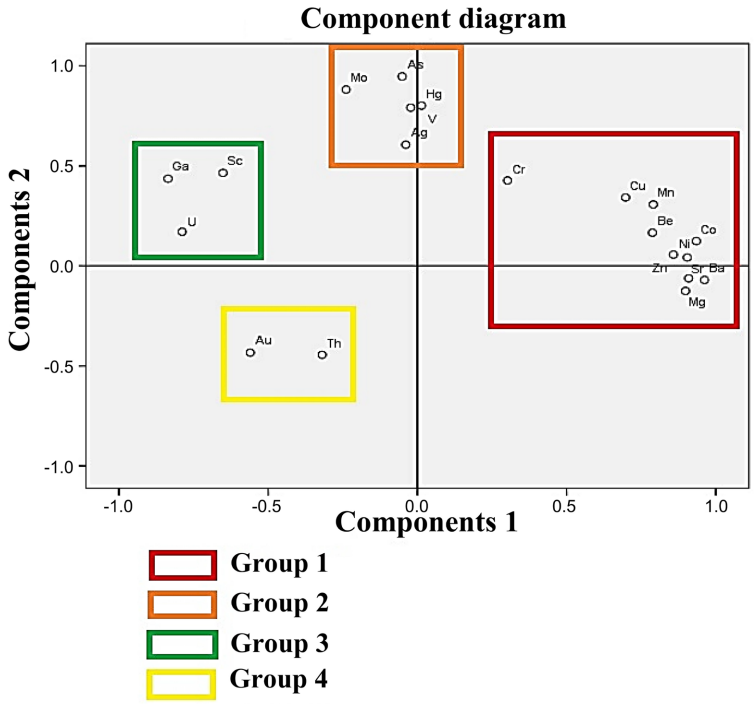

Figure 5. PCA of chemical elements.

The chemical element principal component plot provided the principal component plot of the stream sediment samples along two axes X (REGR factor score 1 for analysis 1) and Y (REGR factor score 2 for analysis 1) (**Figure 6**). Samples EY-10, EY-12, EY-17, and EY-18 are highly enriched on average in Group 1 elements. Samples EY-11 and EY-09 concentrate a very high average in group 2 elements. A high average of group 3 elements is concentrated in samples EY-14 and EY-15. Samples EY-16 and EY-17 concentrate a high average in group 4 elements.

4.5. Rare Earth and Trace Elements

In interpreting the rare earth element distribution, the chondrite-normalized spectrum [20] indicates a high abundance of Lanthanide (28.1 ppm to 42.4 ppm), a high concentration of light rare earth (LREE), and depletion of heavy rare earth (HREE), a flat spectrum of heavy rare earth ranging from Gadnium to lutecium (**Figure 7(A)**). In other words, heavy rare earth and light rare earth have differential mobility in a supergene environment. The elevated rare earth fractionation with increasing (La/Yb)N ratio is directly proportional to the increase in alteration degree [21] [22]. Furthermore, the trace elements of the analyzed samples are normalized to NASC (North American Shale Composite) (**Figure 7(B)**). They show a nearly similar distribution of varying concentrations (peak intensity). The most represented elements are Thorium (Th), Cerium (Ce), Sm, and Europium (Eu). The contrasting behavior of the normalized spectrum of the SINC is because the analyzed samples have high REE contents, in particular REEL, compared to the HREE.

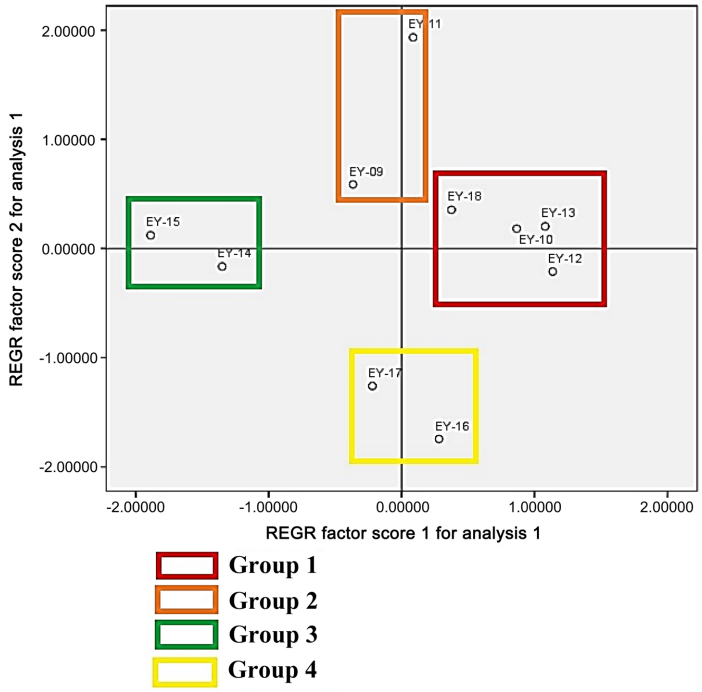

Figure 6. PCA of stream samples.

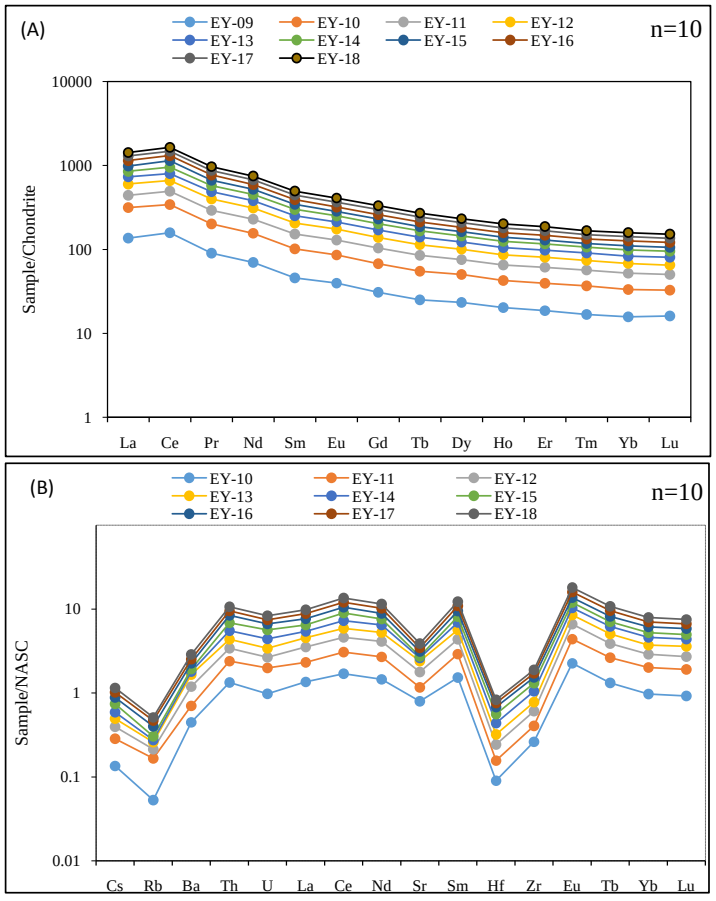

Figure 7. Spectra of chemical elements normalised to chondrites: (A) Rare earths normalized to chondrites; (B) Trace elements normalized to NASC.

5. Discussion

The distribution of trace metals in sediments found that some Lithophiles (Be, Sc, V, Cr, Sr, Th, U), Chalcophiles (Cu, Zn, Ga, As), and Siderophiles (Mn, Co, Ni, Mo) have high average contents in sediments compared to their average concentration in the upper crust [23]. The Pearson correlation coefficient of Mg is high positive with Mn, Ba, Cu, Zn, Co, Sr, Be, and Ni; high negative with U, Ga, Au (Table 5). The high correlation of Mg with Ba shows the presence of pyroxenes, in this case, augite (clinopyroxene) in the sediments from the sub-basin. Generally, scandium (Sc) is associated with ferromagnesian rocks such as peridotites and pyroxenites. The negative correlation between Sc and Mg (r = −0.476) supports this statement. The mafic or ultramafic rocks encountered in the study area could be sources of positive scandium anomalies in stream sediments. Because the V^{+3} ion is nearly identical to Fe^{+3}, V is found as a minor constituent in Fe-bearing minerals. The distribution of V in stream sediments may be related to the presence of pyroxenes [24]. The average V content is higher than the average of [19] and [25], threshold value, and V in ferralitic soils. The

Table 5. Pearson correlation coefficient table.

	Cr	Mg	Mn	Ba	Mo	Cu	Zn	Ag	Ni	Co	As	U	Au	Th	Sr	V	Sc	Hg	Ga	Be
Cr	1																			
Mg	0.149	1																		
Mn	0.38	**0.568**	1																	
Ba	0.259	**0.943****	**0.744***	1																
Mo	0.324	−0.275	−0.031	−0.252	1															
Cu	0.163	**0.644***	0.461	**0.568**	0.167	1														
Zn	0.232	**0.817****	**0.582**	**0.874****	−0.164	**0.727***	1													
Ag	0.214	−0.321	0.207	−0.201	0.352	0.115	−0.094	1												
Ni	**0.660***	**0.656***	**0.742***	**0.783****	−0.217	**0.522**	**0.761***	0.127	1											
Co	0.207	**0.780****	**0.888****	**0.874****	−0.182	**0.718***	**0.840****	0.096	**0.784****	1										
As	0.387	−0.211	0.280	−0.093	**0.921****	0.228	−0.026	0.550	−0.001	0.087	1									
U	−0.372	**−0.794**	**−0.519**	**−0.764**	0.299	−0.450	**−0.623**	0.251	**−0.682**	**−0.589**	0.276	1								
Au	−0.006	**−0.545**	−0.345	**−0.523**	−0.270	**−0.695**	**−0.549**	−0.345	−0.346	**−0.532**	−0.339	0.214	1							
Th	−0.446	−0.311	−0.489	−0.264	−0.227	−0.282	−0.008	−0.121	−0.299	−0.281	−0.245	**0.999****	0.105	1						
Sr	0.194	**0.814****	**0.807****	**0.933****	−0.116	0.550	**0.823****	−0.185	**0.707***	**0.871****	0.069	−0.616	−0.527	−0.213	1					
V	0.472	0.003	0.198	−0.068	**0.738***	0.333	−0.165	0.164	0.005	0.010	**0.658***	−0.129	−0.144	**−0.754**	−0.024	1				
Sc	−0.275	−0.476	−0.422	**−0.569**	**0.694***	−0.190	**−0.580**	−0.075	**−0.772**	**−0.540**	**0.506**	**0.621**	0.068	0.025	−0.412	0.494	1			
Hg	0.173	−0.137	0.342	−0.072	**0.503**	0.263	−0.102	**0.818****	0.081	0.219	**0.696***	0.323	**−0.509**	−0.243	−0.016	0.419	0.222	1		
Ga	0.070	**−0.782**	**−0.520**	**−0.775**	**0.647***	**−0.513**	**−0.746**	0.154	**−0.637**	**−0.749**	**0.508**	**0.774****	0.323	0.168	**−0.656**	0.355	**0.794****	0.264	1	
Be	0.042	**0.646***	**0.638***	**0.779****	0.086	**0.581**	**0.836****	0.081	**0.531**	**0.770****	0.257	−0.425	**−0.691**	0.000	**0.865****	−0.109	−0.305	0.105	**−0.559**	1

*correlation is significant at the 0.05 level (bilateral). **correlation is significant at the 0.01 level (bilateral).

positive correlations between Cr: Mn, Cr: Mg, and Cr: Zn could be the reason for the formation of chromites. This anomalous Cr enrichment may be preferentially due to the high contents of ferromagnesian elements in olivine and pyroxene reported by Edima in 2020, in olivine-pyroxene basalts and peridotites from the Nyambaka locality. The average Cr content is higher than the average of [19] [25] [26] [27]. Potassium feldspars and micas are the main carriers of Ba [24]. The K contents present in the sample analysis results may be responsible for Ba distribution.

The high correlation of Ni with ferromagnesium minerals may be associated with iron-magnesium-rich ultramafic or mafic rocks, typically intrusive from the lower crust. The weak correlation between Au: U and Au: Th shows that the gold contents could be due to the presence of hydrothermal fluids during the formation of mafic rocks. Zn and Mg could be related to magnetite because Zn shows a tendency to be incorporated into oxides by replacing Fe^{+2} and Mg^{+2} [28]. The phenomena of arsenic adsorption by manganese oxides are intimately linked to processes of arsenic oxidation and manganese reduction [29], which explains the positive correlation between As and Mn.

Factor 1 in the Factor Analysis highlights a correlation that influences the behavior of Ba and Sr that commonly occupy the feldspar structure [30]. Mg being associated with magnetite and olivine minerals. Factor 3 indicates that some chalcophile (Hg, Ag) could be found around gold indications that may be mineralization of quartz and gold veins by sulfide reflection. Factors 4 and 5 account for 8.147% and 5.111% of the total variability respectively. These factors showed high and positive loadings of V, Ni, and Cr (**Table 3**). The sediments could be derived from granitic rocks or some felsic rocks and even metasedimentary rocks such as quartzites and amphibolites [19]. The dispersion of Group 1 elements in the principal component factor analysis is opposite to Group 3 elements. This shows that stream sediments rich in Group 1 elements are depleted in Group 3 elements. Similarly, Group 2 element contents are opposite to Group 4 elements, hence Group 2 element-rich stream sediments are depleted in Group 4 elements. However, some Group 2 elements are found at high contents in Group 1 element-rich sediments (**Figure 5**). On the other hand, we note that the contents of elements of groups 3 and 4 are low in the samples. These samples concentrate high levels of group 1 and 2 elements.

The variable LREE/HREE and (La/Yb)N ratios (**Table 6**) may suggest an effect of heterogeneous sorting of heavy minerals with variable enrichment of dense and resistant minerals [31] [32]. The variable LREE/HREE and (La/Yb)N ratios are related to the variable nature of REE mineral carriers. Low LREE/HREE ratios lead to low (La/Yb)N ratios [33]. The low Th/Sc ratios (~0.5) in the Nyambarka alluvial sediments suggest a low degree of sediment recycling. The Th/Sc ratio is an indicator of chemical differentiation, which is controlled by the level of sediment recycling [34]. The low levels of Rb, Ba, and Sr may result from their high mobility.

Table 6. Rare earth element contents (ppm) of alluviums.

	EY-09	EY-10	EY-11	EY-12	EY-13	EY-14	EY-15	EY-16	EY-17	EY-18
La	32.2	42.4	29.8	37.8	31.3	28.1	31.7	3.7	35.8	30.3
Ce	96.6	113.2	91.9	102.5	86	92.5	115.6	102.9	102	99.5
Pr	8.55	10.61	8.55	10.07	8.53	8.31	8.73	9.77	9.52	9.04
Nd	32.66	40.09	34.11	38.49	32.25	33.14	31.58	34.49	37.18	34.3
Sm	7.01	8.53	7.81	8.09	7.16	7.24	6.71	7.37	8.13	7.62
Eu	2.3	2.68	2.52	2.61	2.24	2.21	1.89	2.1	2.68	2.44
Gd	6.34	7.53	7.49	7.14	6.56	6.65	5.5	6.2	8.04	6.67
Tb	0.94	1.12	1.12	1.07	0.99	0.98	0.75	0.95	1.16	1.03
Dy	5.95	6.84	6.45	6.28	5.66	5.63	4.37	5.32	6.47	5.96
Ho	1.15	1.26	1.29	1.17	1.1	1.09	0.82	1.07	1.23	1.23
Er	3.09	3.46	3.61	3.17	2.93	2.98	2.13	3.05	3.22	3,3
Tm	0.43	0.51	0.51	0.44	0.42	0.41	0.28	0.4	0.43	0.43
Yb	2.68	2.98	3.19	2.72	2.56	2.64	1.94	2.77	2.68	2.83
Lu	0.41	0.42	0.45	0.37	0.4	0.37	0.26	0.4	0.37	0.41
ΣREE	200.31	241.63	198.8	221.92	188.1	192.25	212.26	214.49	218.91	205.06
LREE	179.32	217.51	174.69	199.56	167.48	171.5	196.21	194.33	195.31	183.2
HREE	20.99	24.12	24.11	22.36	20.62	20.75	16.05	20.16	23.6	21.86
LREE/HREE	8.54	9.02	7.24	8.92	8.12	8.26	12.22	9.64	8.28	8.38
(La/Yb)N	8.62	10.21	6.70	9.97	8.77	7.63	11.72	9.76	9.58	7.68

6. Conclusions

The geochemical characterization of alluvial sediments from the Nyambaka locality (Adamaoua-Cameroon) was carried out for the geochemical exploration of base metals. The major conclusions are formulated and obtained as follows:

- Lithophiles following, Be, Sc, V, Cr, Sr, Th, U, chalcophiles following Cu, Zn, Ga, As and siderophiles following Mn, Co, Ni, Mo show high average contents in the sediments compared to their average concentration in the upper crust. This seems very interesting for further exploration. Overall, the high trace metal content in stream sediments would be the result of enrichment of the surrounding bedrock and extensive chemical weathering. Thus, the spatial distribution of trace metals is largely controlled by the source geology.
- The component diagram that highlighted the different groups of association between chemical elements in the study area shows that: group 1 elements are opposed to group 3 elements and group 2 elements are opposed to group 4 elements which confirm that the sediments of the creek are much richer in group 1 and 2 elements and less rich in group 3 and 4 elements.
- The high contents of ferromagnesian trace elements such as Cr, V, Ni, and Sc and the depletion of silicic elements such as La, Th show the mafic nature of the source rocks.

Acknowledgements

We thank the Bureau Veritas Laboratory of Canada for geochemical analyses carried out in the framework of this work. Also, we would like to thank Mr. Sounya Boris for his help and advice on the realization of the maps.

Conflicts of Interest

The authors declare no conflicts of interest regarding the publication of this paper.

References

[1] Ujiie-Mikoshiba, M., Imai, N., Terashima, S., Tachibana, Y. and Okay, T. (2006) Geochemical Mapping in Northern Honshu, Japan. *Applied Geochemistry*, **21**, 492-514. https://doi.org/10.1016/j.apgeochem.2005.12.002

[2] Cao, L. and Cheng, Q. (2012) Quantification of Anisotropic Scale Invariance of Geochemical Anomalies Associated with Sn-Cu Mineralization in Gejiu, Yunan Province, China. *Journal of Geochemical Exploration*, **122**, 47-54. https://doi.org/10.1016/j.gexplo.2012.08.001

[3] Meinhold, G., Andres, B., Kostopoulos, D. and Reischmann, T. (2008) Rutile Chemistry and Thermometry as Provenance Indicator: An Example from Chios Island, Greece. *Sedimentary Geology*, **203**, 98-111. https://doi.org/10.1016/j.sedgeo.2007.11.004

[4] Morton, A.C. and Hallsworth, C.R. (1999) Processes Controlling the Composition of Heavy Mineral Assemblages in Sandstones. *Sedimentary Geology*, **124**, 3-29. https://doi.org/10.1016/S0037-0738(98)00118-3

[5] Ahmad, A.H.M., Noufal, K.N., Masroor, A.M. and Tavheed, K. (2014) Petrography and Geochemistry of Jumara Dome Sediments, Kachchh Basin: Implications for Provenance, Tectonic Setting and Weathering Intensity. *Chinese Journal of Geochemistry*, **33**, 9-23. https://doi.org/10.1007/s11631-014-0656-4

[6] Kermani, S., Boutiba, M., Boutaleb, A. and Fagel, N. (2016) Distribution of Heavy and Clay Minerals in Coastal Sediment of Jijel, East of Algeria: Indicators of Sediment Sources and Transport and Deposition Environments. *Arabian Journal of Geosciences*, **9**, Article No. 36. https://doi.org/10.1007/s12517-015-2155-2

[7] Silva, M.V.M.G., Pinto, M.M.S.C. and Carvalho, P.C.S. (2016) Major, Trace and REE Geochemistry of Recent Sediments from lower Catumbela River (Angola). *Journal of African Earth Sciences*, **115**, 203-217. https://doi.org/10.1016/j.jafrearsci.2015.12.014

[8] Ekoa Bessa, A.Z., Ngueutchoua, G. and Ndjigui, P.D. (2018) Mineralogy and Geochemistry of Sediments from Simbock Lake, Yaoundé Area (Southern Cameroon): Provenance and Environmental Implications. *Arabian Journal of Geosciences*, **11**, Article No. 710. https://doi.org/10.1007/s12517-018-4061-x

[9] Nforba, M.T., Kamgang, K.V. and Suh, C.E. (2011) Regolith Geochemistry and Mineralogy of the Mbalam Itabirite Hosted Iron Ore District, South Eastern Cameroon. *Open Journal of Geology*, **1**, 17-36. https://doi.org/10.4236/ojg.2011.12003

[10] Cohen, D.R., Silva-Santisteban, C.M., Rutherford, N.F., Garnett, D.L. and Waldron, H.M. (1999) Comparison of Vegetation and Stream Sediment Geochemical Patterns in Northeastern New South Wales. *Journal of Geochemical Exploration*, **66**, 469-489. https://doi.org/10.1016/S0375-6742(99)00042-4

[11] Briggs, P.L. and Press, F. (1977) Pattern Recognition Applied to Uranium Prospecting. *Nature*, **268**, 125-127. https://doi.org/10.1038/268125a0

[12] Xie, X., Liu, D., Xiang, Y., Yan, G. and Lian, C. (2004) Geochemical Blocks for Predicting Large Ore Deposits-Concept and Methodology. *Journal of Geochemical Exploration*, **84**, 77–91. https://doi.org/10.1016/j.gexplo.2004.03.004

[13] Chiprés, J.A., Salinas, J.C., Castro-Larragoitia, J. and Monroy, M.G. (2008) Geochemical Mapping of Major and Trace Elements in Soils from the Altiplano Potosino, Mexico: A Multiscale Comparison. *Geochemistry: Exploration, Environment, Analysis*, **8**, 279-290. https://doi.org/10.1144/1467-7873/08-181

[14] Edima Yana, R.W., Bidjo Emvoutou, G.C., Okomo Atouba, L.C., Ondoua Oyono, J.S., Ipan, A.S., Sep Nlomngan, J.P. and Nkouandou, F.O. (2021) Stream Sediments Geochemistry of the Nyambaka Drainage System Northern Cameroon (Central Africa): A Target for Mining Exploration. *International Journal of Statistical Distributions and Applications*, **7**, 25-34. https://doi.org/10.11648/j.ijsd.20210702.11

[15] Armstrong-Altrin, J.S., Lee, Y.I., Kasper-Zubillaga, J.J., Carranza-Edwards, A., Garcia, D., Eby, G.N., Balaram, V. and Cruz-Ortiz, N.L. (2012) Geochemistry of Beach Sands along the Western Gulf of Mexico, Mexico: Implication for Provenance. *Geochemistry*, **72**, 345-362. https://doi.org/10.1016/j.chemer.2012.07.003

[16] Ngako, F., Jegouzo, P. and Nzenti, J.P. (1991) Le Cisaillement Centre Camerounais. Rôle structural et géodynamique dans l'orogenèse panafricaine. *Comptes Rendus de l'Académie des Sciences*, **313**, 457-463.

[17] Ngangom, E. (1983) Étude tectonique du fossé Crétacé de la Mbéré et du Djérem, Sud-Adamawa, Cameroun. *Bulletin des Centres de Recherches Exploration—Production Elf-Aquitaine*, **7**, 339-347.

[18] Toteu, S.F., Van Schmus, R.W., Penaye, J. and Michard, A. (2001) New U-Pb and Sm-Nd Data from North Central Cameroon and Its Bearing on the Pre-Pan-African History of Central Africa. *Precambrian Research*, **108**, 45-73. https://doi.org/10.1016/S0301-9268(00)00149-2

[19] Mimba, M.E., Takeshi, O., Nguemhe, F.S.C., Nforba, M.T., Nozomi, N., Bafon, T.G., Aka, T.F. and Suh, C.E. (2018) Regional Geochemical Baseline Concentration of Potentially Toxic Trace Metals in the Mineralized Lom Basin, East Cameroon: A Tool for Contamination Assessment. *Geochemical Transactions*, **19**, 11. https://doi.org/10.1186/s12932-018-0056-5

[20] Pourmand, A., Dauphas, N. and Ireland, T.J. (2012) A Novel Extraction Chromatography and MC-ICP-MS Technique for Rapid Analysis of REE, Sc and Y: Revising CI-Chondrite and Post Archean Australian Shale (PAAS) Abundances. *Chemical Geology*, **291**, 38-54. https://doi.org/10.1016/j.chemgeo.2011.08.011

[21] Ma, J.L., Wei, G.J., Xu, Y.G., Long, W.G. and Sun, W.D. (2007) Mobilization and re-Distribution of Major and Trace Elements during Extreme Weathering of Basalt in Hainan Island, South China. *Geochimica et Cosmochimica Acta*, **71**, 3223-3237. https://doi.org/10.1016/j.gca.2007.03.035

[22] Yusoff, Z.M., Ngwenya, B.T. and Parsons, I. (2013) Mobility and Fractionation of REEs during Deep Weathering of Geochemically Contrasting Granites in a Tropical Setting, Malaysia. *Chemical Geology*, **349**, 71-86. https://doi.org/10.1016/j.chemgeo.2013.04.016

[23] Rudnick, R.L. and Gao, S. (2004) Composition of the Continental Crust. In: Rudnick, R.L., Ed., *Treatise on Geochemistry*, *Vol.* 3, *The Crust*, Elsevier-Pergamon, Oxford, 1-64. https://doi.org/10.1016/B0-08-043751-6/03016-4

[24] Pulchelt, H. (1978) Barium: Abundance in Rock Forming Minerals (I) and Barium

Minerals (II). In: Wedepohl, K.H., Ed., *Hand Book of Geochemistry*, *Vol. II/4*, Springer, Berlin, 56D-1-56D-18.

[25] Towett, E.K., Shepherd, K.D., Tondoh, J.E., Winowiecki, L.A., Lulseged, T., Nyambura, M., Sila, A., Vagen, T.G. and Cadisch, G. (2015) Total Elemental Composition of Soils in Sub-Saharan Africa and Relationship with Soil Forming Factors. *Geoderma Regional*, **5**, 157-168. https://doi.org/10.1016/j.geodrs.2015.06.002

[26] Tehna, N., Nguene, F.D., Etame, J., Medza Ekodo, J.M., Noa, T.S., Suh, C.E. and Bilong, P. (2015) Impending Pollution of Betare Oya Opencast Mining Environment (Eastern Cameroon). *Journal of Environmental Science and Engineering*, **4**, 37-46. https://doi.org/10.17265/2162-5263/2015.01.006

[27] Manga, V.E., Neba, G.N. and Suh, C.E. (2017) Environmental Geochemistry of Mine Tailings Soils in the Artisanal Gold Mining District of Bétaré-Oya, Cameroon. *Environmental Pollution*, **6**, 52-61. https://doi.org/10.5539/ep.v6n1p52

[28] Wedepohl, K.H. (1978) Manganese: Abundance in Rock Forming Minerals, Phase Equilibria, Manganese Minerals. In: Wedepohl, K.H., (Ed), *Hand Book of Geochemistry*, *Vol. II/4*, Springer, Berlin, 25-26.

[29] Nesbitt, H.W., Canning, G.W. and Bancroft, G.M. (1998) XPS Study of Reductive Dissolution of 7Å-Birnessite by H_3AsO_3, with Constraints on Reaction Mechanism. *Geochimica et Cosmochimica Acta*, **62**, 2097-2110. https://doi.org/10.1016/S0016-7037(98)00146-X

[30] Freyssinet, P.H., Lecompte, P. and Edimo, A. (1989) Dispersion of Gold Base Metals in the Mborguene Lateritic Profile, East Cameroon. *Journal of Geochemical Exploration*, **32**, 99-116. https://doi.org/10.1016/0375-6742(89)90050-2

[31] Kasanzu, C., Maboko, M.A.H. and Manya, S. (2008) Geochemistry of Finegrained Clastic Sedimentary Rocks of the Neoproterozoic Ikorongo Group, NE Tanzania: Implications for Provenance and Source Rock Weathering. *Precambrian Research*, **164**, 201-213. https://doi.org/10.1016/j.precamres.2008.04.007

[32] Nyobe, J.M., Sababa, E., Bayiga, E.C. and Ndjigui, P.D. (2018) Mineralogical and Geochemical Features of Alluvial Sediments from the Lobo Watershed (Southern Cameroon): Implications for Rutile Exploration. *Comptes Rendus Geoscience*, **350**, 119-129. https://doi.org/10.1016/j.crte.2017.08.003

[33] Li, Q., Liu, S., Han, B., Zhang, J. and Chu, Z. (2005) Geochemistry of Metasedimentary Rocks of the Proterozoic Xingxingxia Complex: Implications for Provenance and Tectonic Setting of the Eastern Segment of the Central Tianshan Tectonic Zone, Northwestern China. *Canadian Journal of Earth Sciences*, **42**, 287-306. https://doi.org/10.1139/e05-011

[34] McLennan, S.M., Hemming, S., McDaniel, D.K. and Hanson, G.N. (1993) Geochemical Approaches to Sedimentation, Provenance, and Tectonics. In: Johnsson M.J. and Basu, A., Eds., *Processes Controlling the Composition of Clastic Sediments*, Geological Society of America, Boulder, 21-40. https://doi.org/10.1130/SPE284-p21